Supplementary Information (SI) for New Journal of Chemistry.

Synergistic Charge Transfer and Proton Enrichment in Pt/PDDA-Modified CNTs for Enhanced Hydrogen Evolution Reaction

Yuxue Dai,[a,e*] Dayong Song,[a] Mingju Wang,[c] Lianyu Zhang,[a] Yong Zhang,[a] Wenwen Liu,[b*] Xuejing Liu,[d] Chuannan Luo,[d]

1. Experimental section

1.1. Reagents and Solutions.

$H_2PtCl_6 \cdot 6H_2O$ (AR, Pt≥37.5%), sodium borohydride ($NaBH_4$, 99.99%), poly-(dimethyl diallyl ammonium chloride) (PDDA, 20%), nafion solution (5 %) were purchased from Aladdin (Shanghai, China). Multiwall carbon nanotubes (MWCNTs, diameter: 20-40 nm) were purchased from Shenzhen Nanotech Port. Ltd. All other chemicals were of analytical reagents grade and used without further purification. Ultra-pure water (18.25 MΩ cm, 25 °C) was used for the whole experiment.

1.2. Equipment.

All electrochemical measurements were performed on a CHI 760D electrochemical workstation (Shanghai CH Instruments Co., China). Electrochemical impedance spectroscopy (EIS) was obtained from the impedance measurement unit (IM6e, ZAHNER elektrik, Germany). Scanning electron microscope (SEM) was recorded by JSM-6700F microscope (Japan). High-resolution transmission electron microscopy (HRTEM) was recorded from using a JEOL JEM-2100f (Tokyo, Japan). X-ray photoelectron spectroscopy (XPS) was obtained from Thermo ESCALAB 250XI XPS (American). Diffuse reflectance ultraviolet-visible light spectra were measured on a X-Ray Diffraction (XRD) was recorded from (XRD Foucs D8 Brooke AXS Co. Ltd., Germany). Raman spectra were detected on a Renishaw micro-Raman system at an excitation wavelength of 532 nm. Fourier transform infrared spectroscopy (FT-IR) was recorded from FT-1760X (Waters, American). Inductively Coupled Plasma Mass Spectrometry (ICP-MS) was recorded from PerkinElmer NexION 300X (American).

1.3. Preparation of pCNTs

To synthesize poly dimethyl diallyl ammonium chloride (PDDA) modified carbon nanotubes denoted as pCNTs, the commercial MWCNTs were firstly refluxed in concentrated nitric acid to obtain -COOH functional CNTs. CNTs were obtained through centrifugation and washing with water until near neutral and vacuum dried at 60 °C. Then 150 mg of CNTs were dispersed in 50 mL H_2O with ultrasonication for 1 h. Subsequently, 10 mL 2 mg/mL PDDA solution dispersed in water was added to the above solution. After sonication for 30 min, pCNTs were finally obtained *via* vacuum-filtration, washing with water and dried at 60 °C.

1.4. Preparation of EG-Pt/pCNTs hybrid catalysts

According to previous report with a little modification,[1] 20 mg of pCNTs was dispersed in 20 mL of ethylene glycol (EG) with stirring for 1 h. Subsequently, different amounts of H_2PtCl_6 aqueous solution (Pt content = 5 mg/mL) including 20 μL, 60 μL, 100 μL and 200 μL was added to the above solution, respectively. Then the mixed solution was kept at 150 °C for 3 h under the protection of Ar atmosphere. Finally, EG-Pt/pCNTs were obtained after centrifugation and washing with water/ethanol thoroughly and drying at 60 °C. EG treated pCNTs (EG-pCNTs) was also prepared through the similar method without the addition of H_2PtCl_6.

1.5. Preparation of Pt/pCNTs hybrid catalysts

Firstly, 20 mg of pCNTs was dispersed in 20 mL of water. Then 20 μL of H_2PtCl_6 aqueous solution was added to the obtained solution under stirring. After 3 h, 3 mL of the freshly prepared $NaBH_4$ aqueous solution (containing 95 mg $NaBH_4$) was quickly added. After reacting for 3 h, the solution was centrifuged and washed with water/ethanol for 3 times respectively. Finally, Pt/pCNTs were obtained after drying at 60 °C

1.6. Electrochemical measurements

Electrochemical measurements were performed with a three-electrode setup with a saturated calomel electrode (SCE) as the reference electrode and a platinum electrode as the counter electrode, a glassy carbon electrode (GCE, 4 mm in diameter) as the working electrode. The catalyst suspension was prepared by dispersing 5 mg of various catalysts into 1 mL of the mixed solvent containing 200 μL of water, 800 μL of ethanol and 20 μL of 5% Nafion solution. For the preparation of the catalytic electrodes, 5 μL of the catalyst suspension was dropped onto GCE and dried at room temperature naturally. Linear sweep voltammetry (LSV) profiles were employed to investigate the HER activities of various electrodes with a scan rate of 5 mV/s in 1 mol/L KOH and 0.5 mol/L H_2SO_4 solution, respectively. All data were corrected for iR loss unless otherwise noted. The catalytic stability of the electrodes was recorded as a function of reaction time. Before the electrochemical test, E(RHE) = E(SCE) + 1.023 +0.059pH V for 1 mol/L KOH electrolyte and E(RHE) = E(SCE)+0.242+0.059pH for 0.5 mol/L H_2SO_4 electrolyte.

The electrochemical double-layer capacitance (C_{dl}) was determined from cyclic voltammograms measured in a non-Faradaic region at different scan rates (v = 40, 60, 80, 100 and 120 mV/s) in the potential range 0.07 to 0.17 V versus RHE. The current differences at 0.12 V against scan rates were fitted to obtainthe C_{dl}: $C_{dl} = I_c/v$, where C_{dl}, I_c, and v are the double-layer capacitance (mF/cm^2) of the electroactive materials, charging current (mA/cm^2), and scan rate (mV/s).

Electrochemical impedance spectra (EIS) experiments were performed with the three-electrode cell system in 0.5 mol/L H_2SO_4 solution at 25 °C. The amplitude of the sinusoidal wave was 10 mV, and the frequency scan range was from 10 kHz to 100 mHz. The experimental data were fitted to the equivalent circuit by ZsimpWin software.

It is possible to use the fitting and simulation tool to simplify a parallel combination of a resistor and a constant phase element (*CP*E) by converting the *CPE* to pseudocapacitance *C*, according to Eq. (1):

$$C = Y_0^{1/n} \cdot R^{(1/n)-1} \quad (1)$$

where C is the pseudocapacitance, Y_0 is the admittance value of the constant phase element, R is the resistance value and n is the exponent of the constant phase element.

1.7. Computational methods and details

DFT calculations were carried out using the PWSCF (planewave self-consistent field) plane-wave code in the open-source Quantum ESPRESSO package, using the scalar relativistic PAW pseudopotentials.[2-4] The exchange and correlation function was described by the spin-polarized generalized gradient approximation (GGA) with Perdew-Burke-Ernzerhof (PBE)[5] and the cutoff of kinetic energy for the description of the wave function were set to 35 Ry. The atomic positions were optimized until the force on each atom was less 0.03 eV/Å while self-consistent iteration on the electronic wave function was performed with a convergence criterion of 1.0×10^{-6} Ry. The vacuum layer of 20 Å thickness was set to avoid the periodic interaction. The Monkhorst−Pack *k*-points used in the structural optimization and calculations of electrons property were 2 × 2 × 1 and 4 × 4 × 1, respectively.[6] Van der Waals (vdW) correction by Grimme's DFT-D2 method has also been considered.[7, 8] The model system of EG coated Pt nanoparticles supported on the PDDA wrapped CNTs was briefly simulated consisting of one ethylene glycol molecule (EG), Pt(111) with 9 metal atoms, one unit of PDDA polymer electrolyte, and periodically repeating monolayer graphene with 5 × 3 supercell as shown in Fig. 1a and the Pt(111) and graphene surfaces presented the mismatch of 4.59% and 5.86%. The solvation effect was considered by the environ plugin using water as the solvent and the PBC correction was used to help energy convergence of the model system.[9] The Xcrysden[10, 11] and Visualization for Electronical and Structural Analysis (VESTA)[12] programs were utilized for structure model and difference charge density analyses.

2. Results and discussion

Table S1 The actual Pt loadings of as-prepared EG-Pt/pCNTs, Pt/pCNTs and Pt/CNTs catalysts.

Sample	EG-Pt/pCNTs				Pt/pCNTs				Pt/CNTs			
	20	60	100	200	20	60	100	200	20	60	100	200
Calculated Pt loading (wt. %)	0.5	1.5	2.5	5	0.5	1.5	2.5	5	0.5	1.5	2.5	5
Actual Pt loading (wt. %)	0.42	1.38	2.31	4.65	0.44	1.41	2.18	4.91	0.48	1.44	2.37	4.83

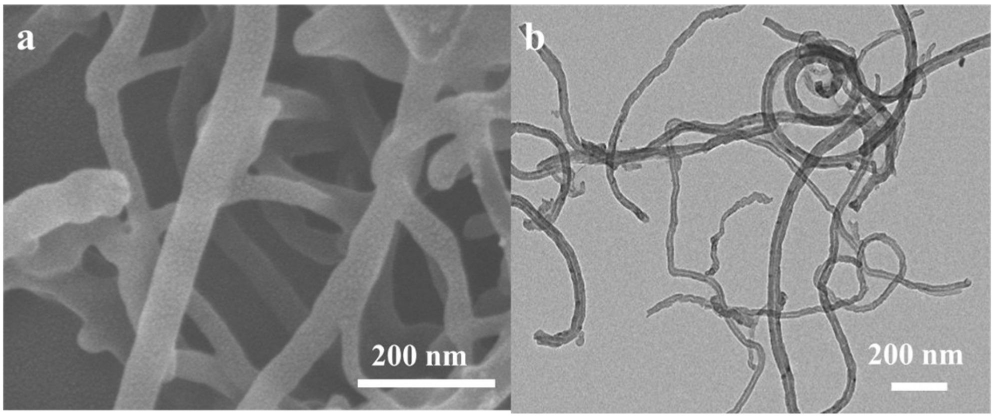

Fig.S1 SEM (a) and TEM (b) images of CNTs.

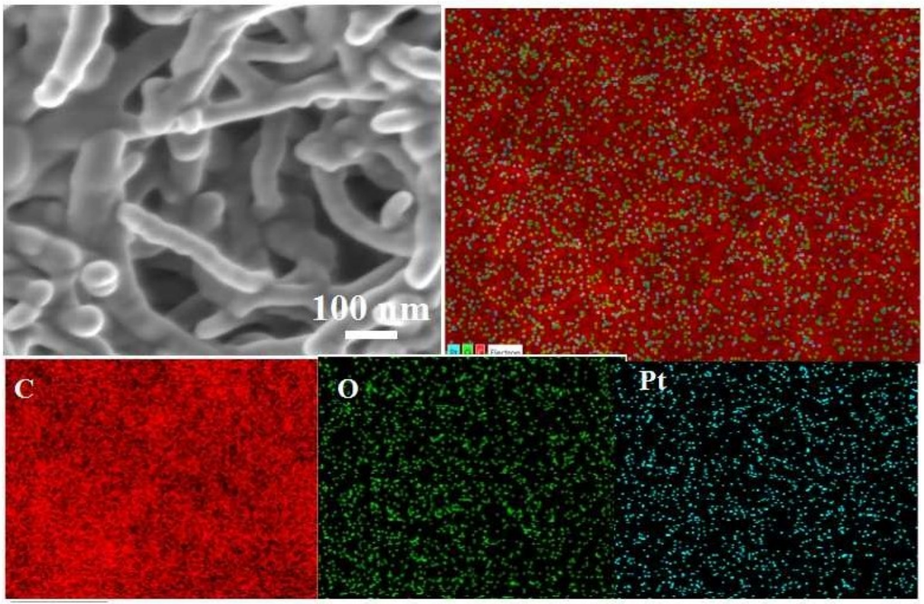

Fig.S2 SEM image and the corresponding EDX elemental mappings for C, O, and Pt of Pt/CNTs.

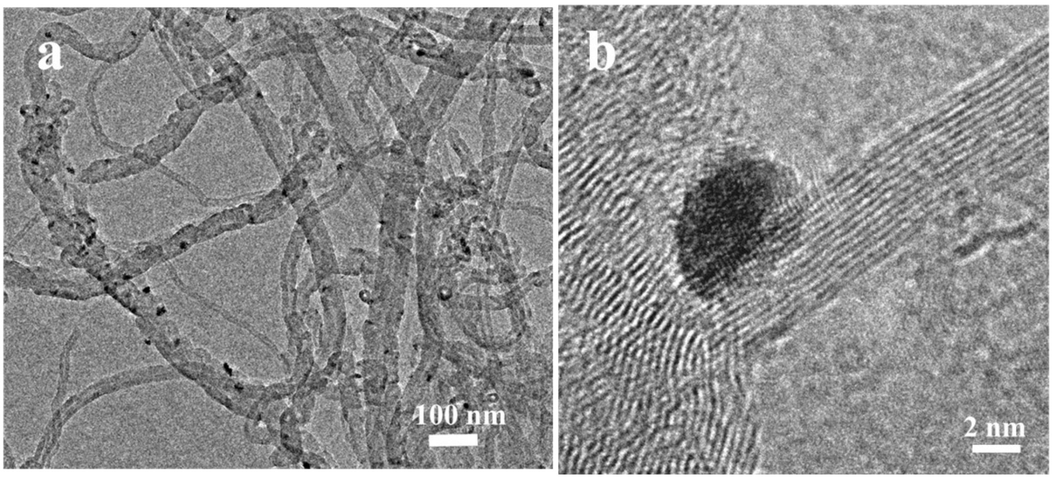

Fig.S3 TEM (a) and HRTEM (b) images of Pt/CNTs.

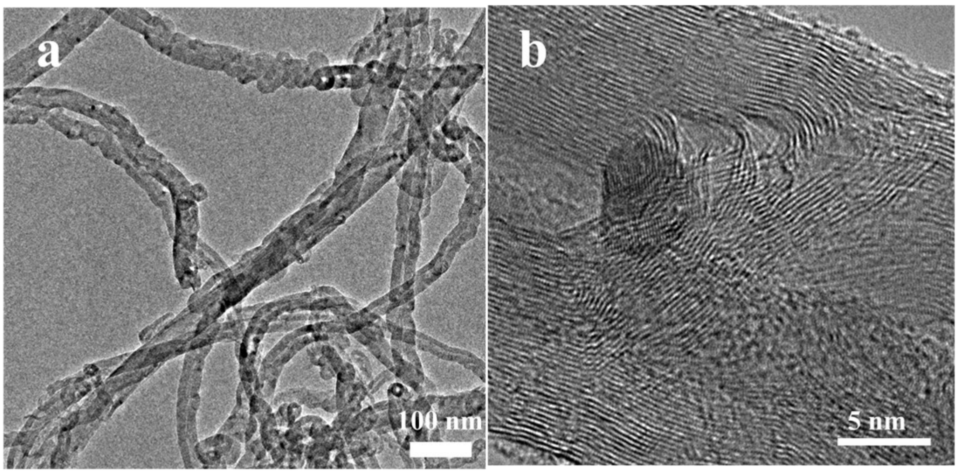

Fig.S4 TEM (a) and HRTEM (b) images of Pt/pCNTs.

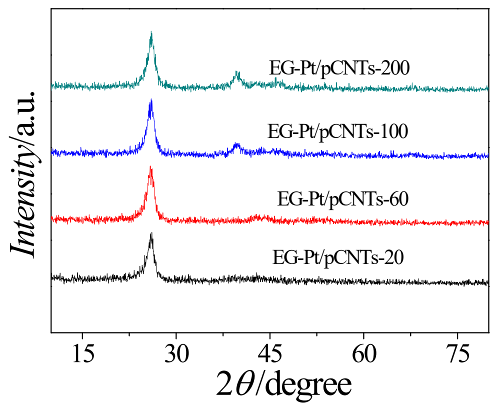

Fig.S5 XRD patterns of EG-Pt/pCNTs-20, EG-Pt/pCNTs-60, EG-Pt/pCNTs-80 and EG-Pt/pCNTs-100.

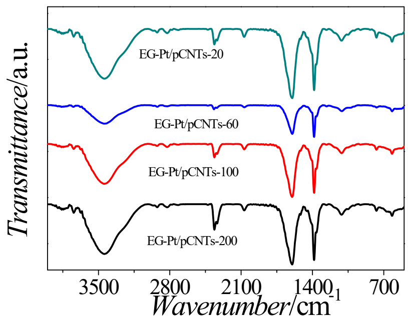

Fig.S6 FT-IR spectrum of EG-Pt/pCNTs-20, EG-Pt/pCNTs-60, EG-Pt/pCNTs-100 and EG-Pt/pCNTs-200.

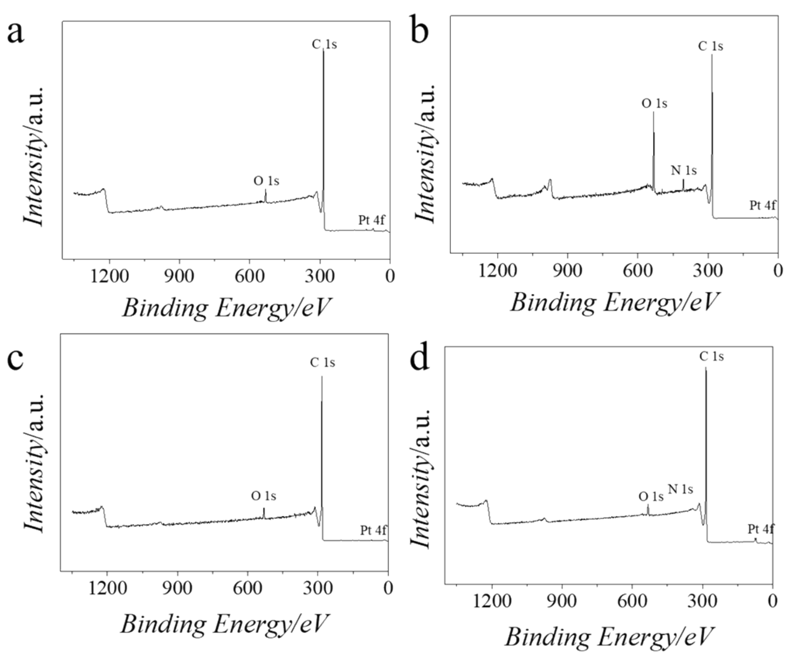

Fig.S7 XPS survey scans of Pt/CNTs (a), Pt/pCNTs (b), EG-Pt/CNTs (c) and EG-Pt/pCNTs (d).

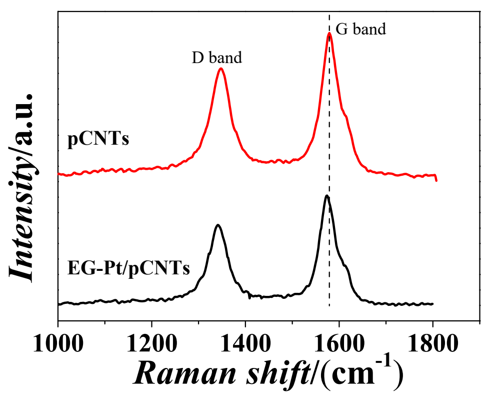

Fig.S8 Raman spectra of pCNTs and EG-Pt/pCNTs.

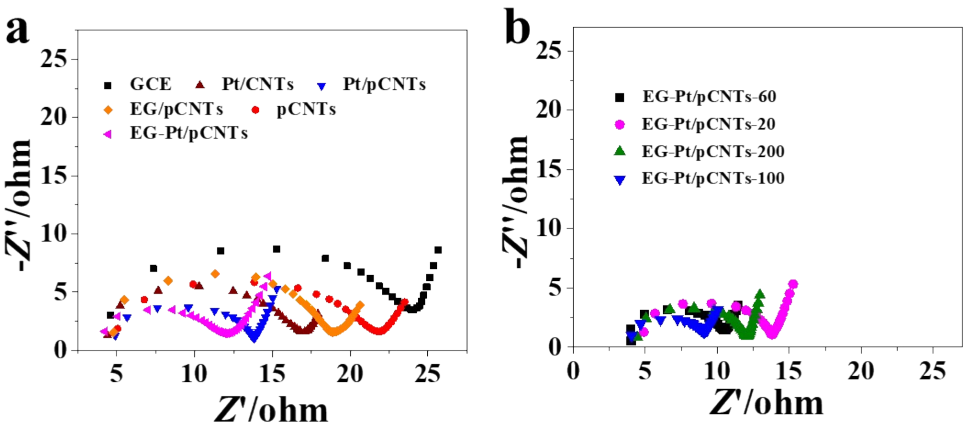

Fig.S9 (a) Nyquist plots of GCE, CNTs, pCNTs, EG/pCNTs, Pt/CNTs, Pt/pCNTs and EG-Pt/pCNTs-20 at open circuit potential. (b) Nyquist plots of EG-Pt/pCNTs-20, EG-Pt/pCNTs-60, EG-Pt/pCNTs-100 and EG-Pt/pCNTs-200 at open circuit potential.

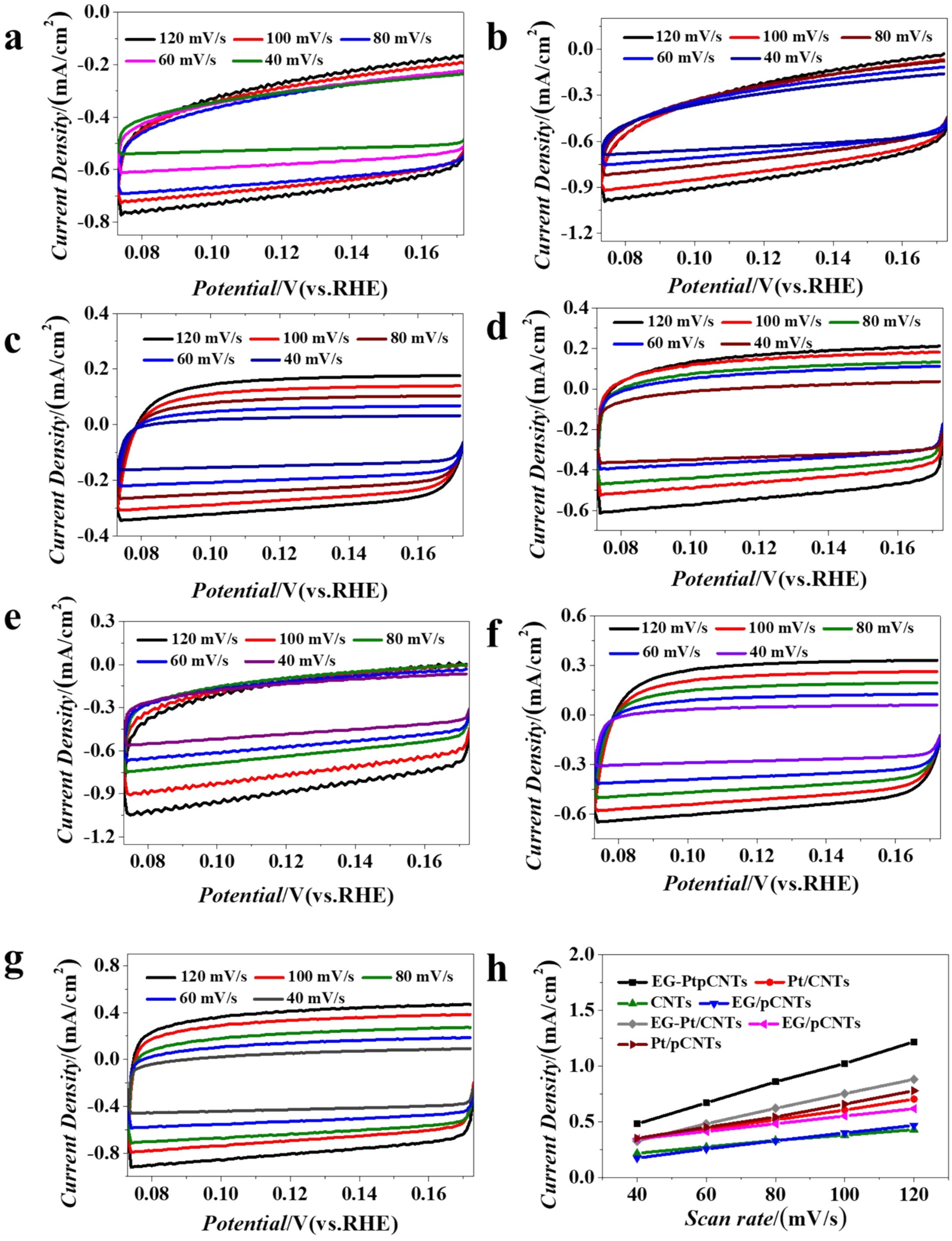

Fig.S10 CV curves of as-prepared catalysts measured in a non-Faradaic region at different scan rates (40-120 mV/s) for estimating the electrochemical double-layer capacitance: CNTs (a), pCNTs (b), EG/pCNTs (c), Pt/CNTs (d), Pt/pCNTs (e), EG-Pt/CNTs (f), EG-Pt/pCNTs-20 (g). (h) linear fitting of the capacitive current densities of CNTs, pCNTs, EG/pCNTs, Pt/CNTs, Pt/pCNTs, EG-Pt/CNTs, EG-Pt/pCNTs-20 at 1.20 V vs. RHE against scan rate.

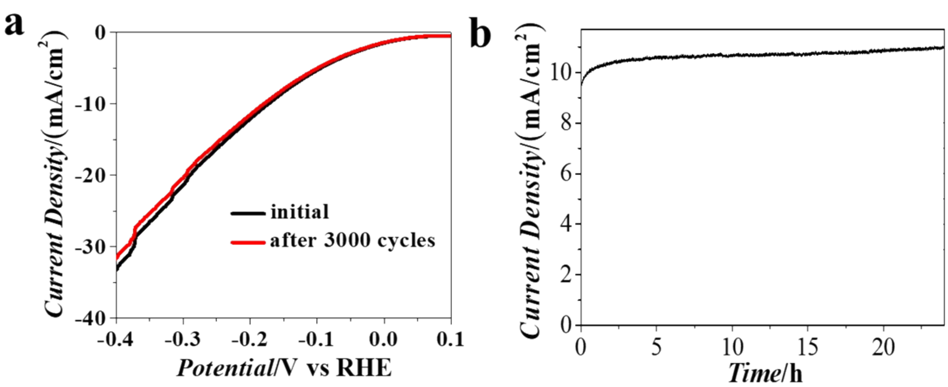

Fig.S11 Stability test of EG-Pt/pCNTs-100 in 1 mol/L KOH. (a) Polarization curves of EG-Pt/pCNTs-100 in 1 mol/L KOH before and after long-term 1000 cycles (0.2 to 0.5 V vs. RHE, 100 mV/s). (b) Current-time curves of EG-Pt/pCNTs-100 measured at an overpotential of 175 mV in 1 mol/L KOH for 24 hours.

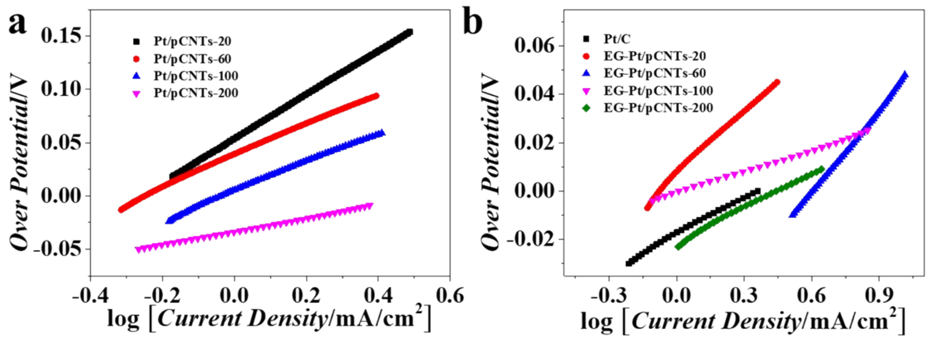

Fig.S12 Tafel slopes derived from the polarization curves of Pt/pCNTs (a) and EG-Pt/pCNTs (b) containing different amounts of Pt measured in 0.5 mol/L H_2SO_4 solution.

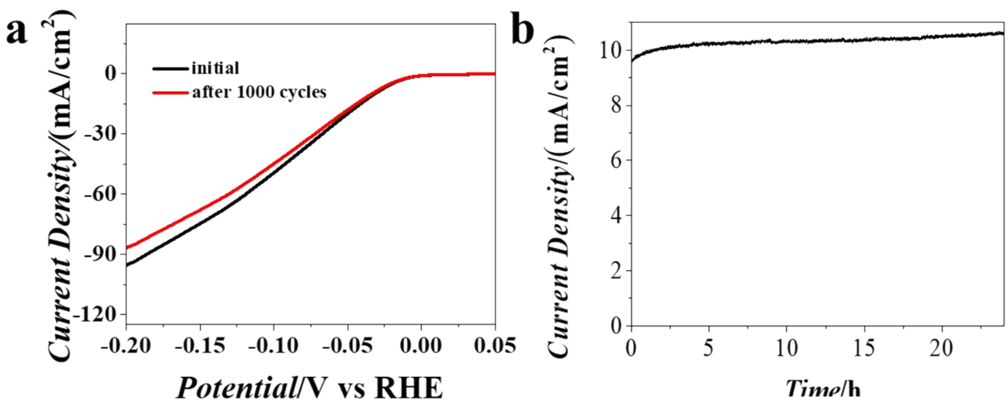

Fig.S13 Stability test of EG-Pt/pCNTs-100 in 0.5 mol/L H_2SO_4 solution. (a) Polarization curves of EG-Pt/pCNTs-100 in 0.5 mol/L H_2SO_4 solution before and after long-term 1000 cycles. (b) Current-time curves of EG-Pt/pCNTs-100 measured at an overpotential of 29 mV in 0.5 mol/L H_2SO_4 solution.

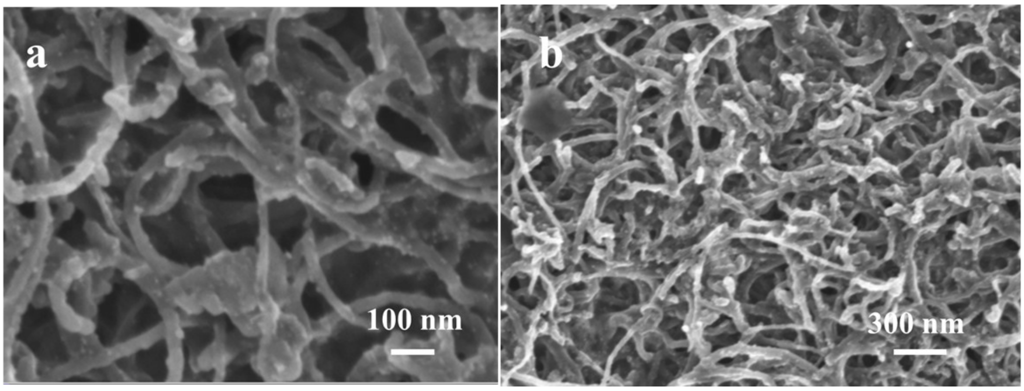

Fig.S14 SEM image of EG-Pt/pCNTs-100 after long-term stability in 0.5 mol/L H_2SO_4 solution (a) and 1 mol/L KOH solution (b).

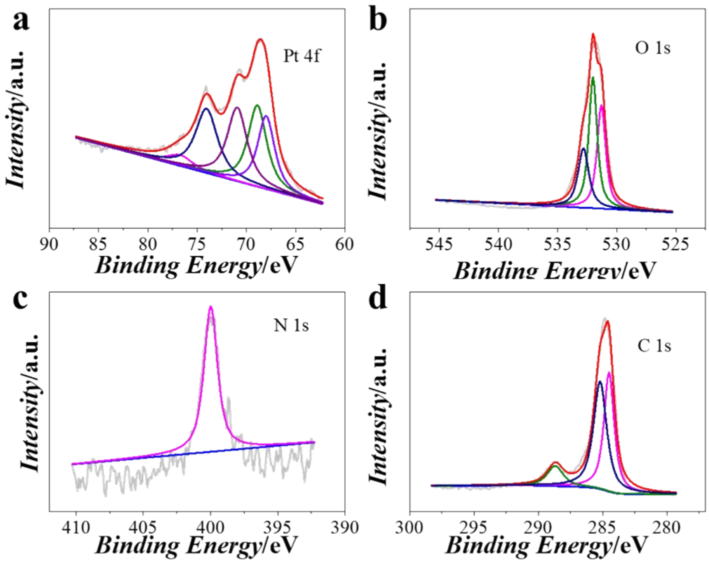

Fig.S15 The high-resolution Pt 4f XPS spectrrum (a), O 1s spectrum (b), N 1s spectrum (c) and C 1s spectrum (d) of EG-Pt/pCNTs-100 after long-term stability in 0.5 mol/L H_2SO_4 solution.

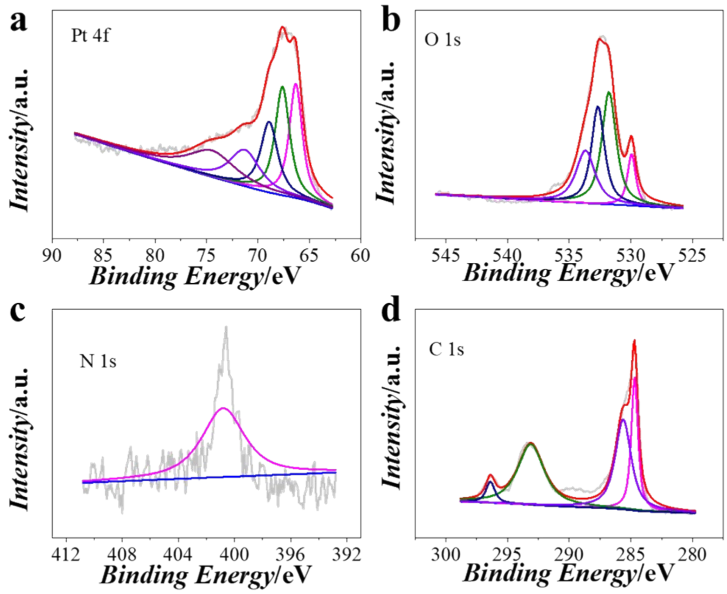

Fig.S16 The high-resolution Pt 4f XPS spectrrum (a), O 1s spectrum (b), N 1s spectrum (c) and C 1s spectrum (d) of EG-Pt/pCNTs-100 after long-term stability in 1 mol/L KOH solution.

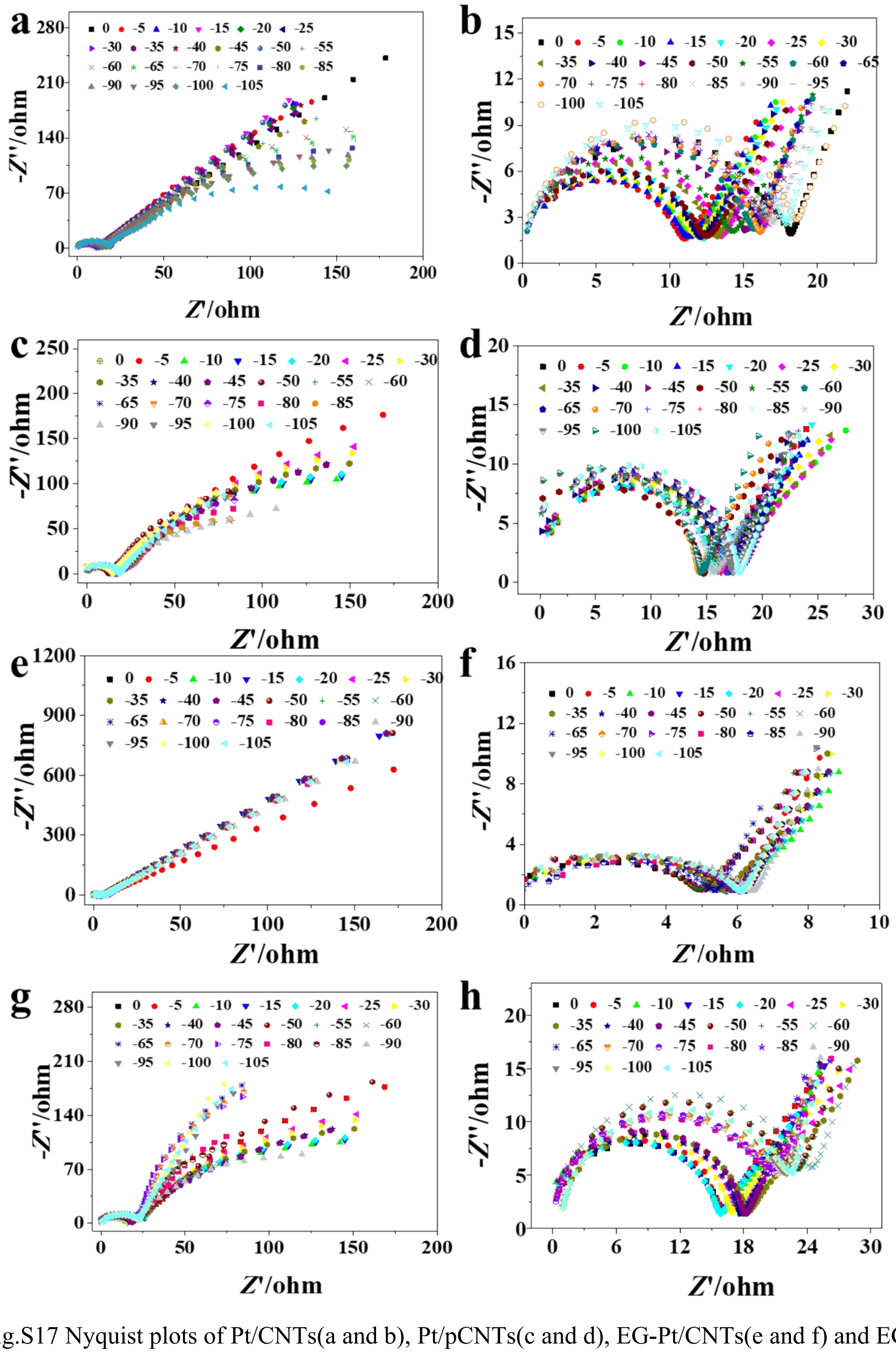

Fig.S17 Nyquist plots of Pt/CNTs(a and b), Pt/pCNTs(c and d), EG-Pt/CNTs(e and f) and EG-Pt/pCNTs-20 (g and h) measured in 0.5 mol/L H_2SO_4 solution at a series of overpotentials ranging from 0 to -105 mV. The left column (a, c, e, g) displayed the full spectrum, while the right column (b, d, f, h) showed the high-frequency region.

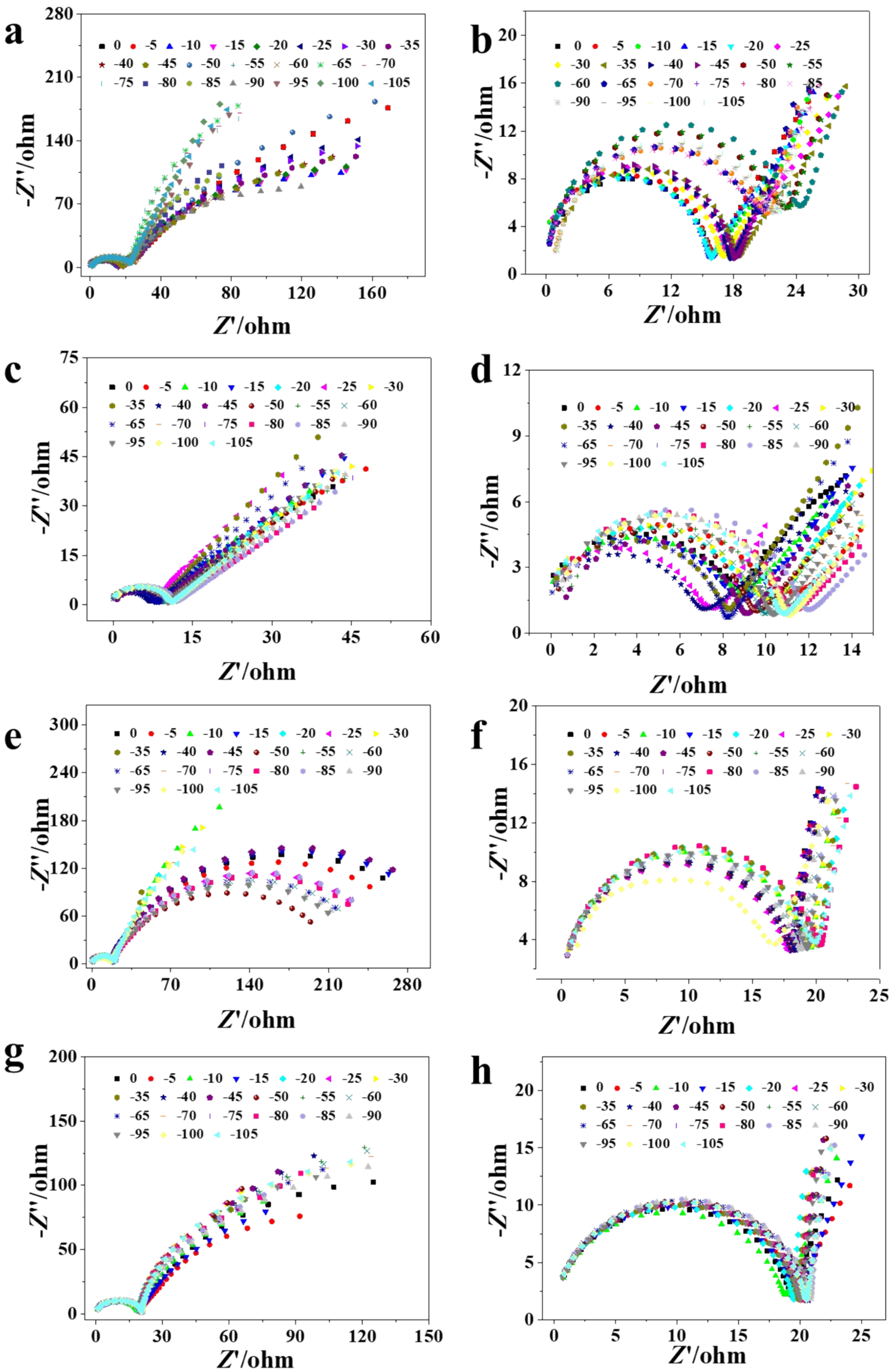

Fig.S18 Nyquist plots of EG-Pt/pCNTs-20 (a and b), EG-Pt/pCNTs-60 (c and d), EG-Pt/pCNTs-100 (e and f) and EG-Pt/pCNTs-200 (g and h) measured in 0.5 mol/L H_2SO_4 solution at overpotentials from 0 to -105 mV. The left column (a, c, e, g) displayed the full spectrum, while the right column (b, d, f, h) showed the high-frequency region.

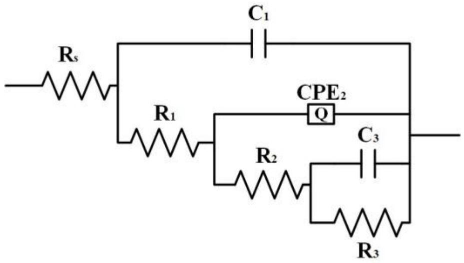

Fig.S19 Equivalent circuits used for fitting of the EIS data of Fig.S17 and Fig.S18. The model comprises: R_s (solution resistance); a R_1-C_1 loop for the primary charge-transfer kinetics; a R_2-CPE$_2$ loop (converted to pseudocapacitance C_2) describing the hydrogen adsorption/desorption process, with the time constant $\tau_2 = R_2 \times C_2$ reflecting its relaxation rate; and a R_3-C_3 loop accounting for surface porosity effects. The use of CPE2 accounts for the non-ideal capacitive behavior of the interface.

Table S2. The fitted parameters of the EIS data of Pt/CNTs-20 for HER.

	η (mV)	R_s (Ω)	C_1 (mF)	R_1 (Ω)	CPE$_2$ (mF)	n	C_2 (mF)	R_2 (Ω)	τ_2/10^{-3}s	C_3 (mF)	R_3 (Ω)
Pt/CNTs	0	5.985	0.0001641	17.84	0.001078	0.6044	0.0811799	0.1304	1.4482	0.03243	3.484E008
	-5	1	0.0003163	10.65	0.001053	0.6941	0.145525	221.6	1.5498	0.08028	1185
	-10	0.01	0.0003321	11.11	0.001405	0.6418	0.13784	46.81	1.5314	0.01006	5.832E015
	-15	0.1	0.0003336	10.82	0.001356	0.6594	0.153177	1.654E015	1.6574	0.000003308	1.221E012
	-20	1	0.0003441	12.05	0.0014	0.639	0.139491	0.1842	1.6809	0.02733	9927
	-25	1	0.0003925	13.35	0.001525	0.6086	0.124624	0.1399	1.6637	0.04714	1E016
	-30	0.1	0.0003424	11.35	0.001368	0.6537	0.150593	8948	1.7092	1.643E+13	1E016
	-35	0.01	0.0003825	12.96	0.001446	0.6248	0.132723	0.1503	1.7201	0.03997	74.69
	-40	0.01	0.0003464	11.75	0.001255	0.6833	0.177768	2.455E006	2.0888	1E+23	1.153E010
	-45	0.01	0.0005244	15.04	0.001493	0.6041	0.124045	0.155	1.8656	0.06116	3357
	-50	10	0.0002969	12.01	0.001411	0.6576	0.168825	1.454E015	2.0276	1E+23	2.795E018
	-55	0.01	0.0004196	13.8	0.001231	0.6889	0.195437	1.137E006	2.6970	1006000000	0.01
	-60	0.1	0.0006635	15.62	0.0005329	0.8342	0.205733	96.19	3.2135	0.3287	304.1
	-65	0.01	0.0009891	16.17	0.0004061	0.887	0.214078	80.69	3.4616	0.4013	257.8
	-70	0.01	0.0006778	16.12	0.0003913	0.9017	0.225248	82	3.6310	0.04067	271.6
	-75	0.01	0.0009777	16.54	0.000351	0.9199	0.224179	7274	3.7079	0.43	242.5
	-80	1	0.001036	16.5	0.0003866	0.8968	0.216093	71.68	3.5655	0.418	225.3
	-85	10	0.001037	16.77	0.0003523	0.9169	0.221277	64.57	3.7108	0.4536	193
	-90	0.1	0.001014	16.98	0.0004309	0.8805	0.221067	68.89	3.7537	0.3938	210.2
	-95	0.01	0.001026	16.11	0.0011	0.7311	0.249565	4.356E006	4.0204	42450000000	2799
	-100	10	0.0009991	18.64	0.0003727	0.9028	0.218272	59.71	4.0686	0.4433	183.3
	-105	0.1	0.001062	18	0.0003045	0.943	0.222286	49.45	4.0011	0.5103	129

Table S3. The fitted parameters of the EIS data of Pt/pCNT-20 for HER.

	η (mV)	R_s (Ω)	C_1 (mF)	R_1 (Ω)	CPE_2 (mF)	n	C_2 (mF)	R_2 (Ω)	$\tau_2/10^{-3}$s	C_2 (F)	R_3 (Ω)
Pt/pCNTs	0	14.78	1.512E-004	15.92	0.0007908	0.7121	0.1349	1033	2.1471	0.0001326	572.4
	-5	14.78	1.512E-004	15.92	0.0007908	0.7121	0.1349	1033	2.1471	0.0001326	572.4
	-10	16.1	1.459E-004	16.5	0.0007617	0.743	0.1676	2598	2.7658	0.000217	261.1
	-15	16.34	1.468E-004	16.22	0.0007336	0.7559	0.1754	32.92	2.8447	0.002141	259.5
	-20	16.51	1.546E-004	16.06	0.0007337	0.7611	0.1820	32.48	2.9232	2.086E-005	268.3
	-25	17.35	1.36E-004	17.88	0.000786	0.7299	0.1622	42.82	2.8999	0.0001867	4008
	-30	17.39	1.42E-004	17.32	0.0007544	0.7478	0.1747	43.71	3.0256	0.0001929	3514
	-35	17.51	1.388E-004	17.6	0.000748	0.746	0.1712	35.31	3.0138	0.002054	311.7
	-40	17.03	1.49E-004	17.48	0.001191	0.7303	0.2850	4.507E004	4.9826	2.505E-016	0.01513
	-45	17.54	1.446E-004	18.34	0.001202	0.7321	0.2976	442.3	5.4584	0.01111	9.472
	-50	0.1	7.506E-005	32.37	0.0005569	0.8451	0.2667	85.19	8.6346	0.0002144	442.6
	-55	0.01	6.548E-005	36.01	0.0006317	0.807	0.2556	45.85	9.2041	2.346E-005	258.4
	-60	10	6.138E-005	37.38	0.0005947	0.8162	0.2524	24.49	9.4337	0.0002482	269.7
	-65	0.01	6.091E-005	38.21	0.0006613	0.7958	0.2573	73.18	9.8329	1.834E-005	508.9
	-70	10	6.091E-005	38.35	0.0006707	0.7987	0.2666	77.26	10.2243	0.0001801	453.1
	-75	10	6.191E-005	37.13	0.0006316	0.8173	0.2730	68.01	10.1352	0.0001982	402.6
	-80	0.1	6.403E-005	36.34	0.0006362	0.8235	0.2838	59.84	10.3117	0.0002038	327
	-85	1000	6.748E-005	34.77	0.0006201	0.8386	0.2963	51.57	10.3029	0.0002211	250.4
	-90	8.72	3.018E-005	70.06	0.0007908	0.654	0.1711	22.97	11.9895	0.0002731	34.67
	-95	10	6.002E-005	38.35	0.001056	0.7486	0.3598	824.2	13.7964	9.745E009	1E016
	-100	100	6.058E-005	38.69	0.001038	0.7563	0.3684	0.01	14.2529	1E-020	1019
	-105	0.01	5.758E-005	39.51	0.00106	0.7499	0.3679	0.01	14.5358	2.569E-020	0.9358

Table S4. The fitted parameters of the EIS data of EG-Pt/CNTs-20 for HER.

	η (mV)	R_s (Ω)	C_1 (mF)	R_1 (Ω)	CPE_2	n	C_2 (mF)	R_2 (Ω)	$\tau_2/10^{-3}$s	C_φ (F)	R_3 (Ω)
EG-Pt/CNTs	0	6.4	3.89E-004	5.622	0.0002194	0.8547	0.070262709	26.65	0.3950	0.0002406	7.496E011
	-5	6.53	3.724E-004	6.287	0.0002398	0.8347	0.066229539	0.01088	0.4164	1.882E-016	1.107E014
	-10	5.691	3.387E-004	6.271	0.0002157	0.851	0.067850809	24.16	0.4255	2.758E-005	9.719E011
	-15	5.843	3.412E-004	5.837	0.0002223	0.8573	0.073521046	27.35	0.4291	0.00246	3.632E012
	-20	5.825	3.284E-004	6.08	0.0002211	0.8546	0.071785371	275	0.4365	2.403E-005	1.441E012
	-25	5.698	3.185E-004	6.23	0.0002179	0.852	0.069213292	2.449	0.4312	2.583E-005	9.962E010
	-30	5.744	3.471E-004	6.015	0.0002222	0.8546	0.072071534	23.22	0.4335	2.543E-005	5.846E019
	-35	5.298	3.071E-004	6.289	0.0002262	0.854	0.07375333	26.97	0.4638	2.435E-006	3.039E013
	-40	5.815	3.392E-004	6.019	0.000224	0.8553	0.073225399	2.775	0.4407	2.39E-005	1.52E013
	-45	5.691	3.202E-004	6.187	0.0002211	0.8584	0.074500676	35.31	0.4609	0.000217	3.145E010
	-50	5.62	3.043E-004	6.273	0.0002189	0.8526	0.070049743	25.33	0.4394	2.494E-005	2.647E019
	-55	5.459	2.967E-004	6.419	0.0002203	0.8514	0.070092385	22.9	0.4499	2.513E-005	2.413E019
	-60	5.672	3.126E-004	6.236	0.0002224	0.8526	0.071292262	24.6	0.4446	0.0002469	1.607E010
	-65	6.76	4.688E-004	5.62	0.0002477	0.8686	0.091585177	73.34	0.5147	6.906E-016	1.386E014
	-70	5.937	3.409E-004	6.153	0.0002503	0.8694	0.094619005	5.281E013	0.5822	324.1	0.01164
	-75	6.177	3.918E-004	5.937	0.0002508	0.8685	0.093599634	2.636E013	0.5557	7.828E-008	2302
	-80	6.332	3.827E-004	5.849	0.0002548	0.8678	0.094532073	6.278E013	0.5529	1E020	0.01424
	-85	6.246	4.072E-004	5.964	0.0002482	0.8695	0.093348773	0.01205	0.5567	1.929E-015	6.927E013
	-90	6.048	3.402E-004	6.355	0.0002504	0.8652	0.091761606	0.01271	0.5831	2.965E-015	1.55E013
	-95	5.417	3.1E-004	6.679	0.0002486	0.8686	0.094401885	2.2E006	0.6305	8.427E-010	1.825E013
	-100	5.668	3.205E-004	6.455	0.0002526	0.8673	0.094604068	1.471E010	0.6107	1.733E-020	1.633E015
	-105	5.362	2.898E-004	6.706	0.000251	0.8687	0.095591034	4.871E013	0.6410	2.699E-009	4.837E005

Table S5. The fitted parameters of the EIS data of EG-Pt/pCNTs-20 for HER.

	η (mV)	R_s (Ω)	C_1 (mF)	R_1 (Ω)	CPE_2	n	C_2 (mF)	R_2 (Ω)	$\tau_2/10^{-3}$s	C_φ (F)	R_3 (Ω)
EG-Pt/pCNTs-20	04	0.8117	1.6E-003	20.85	0.001214	0.446	0.012615503	0.6572	0.2630	8.847E-005	4.486E011
	-5	1	1.606E-003	21.72	0.0009415	0.4883	0.015978866	0.4977	0.3471	0.000103	230.7
	-10	0.01	1.564E-003	22.91	0.0007522	0.5504	0.027269944	0.04914	0.6248	8.838E-005	652.6
	-15	1000	1.52E-003	22.98	0.0007871	0.5475	0.028561583	0.4892	0.6563	8.503E-005	684.3
	-20	0.01	1.411E-003	24.84	0.0008549	0.523	0.02547555	0.5223	0.6328	8.798E-005	869.5
	-25	0.01	1.753E-003	21.1	0.0006752	0.5735	0.028601491	0.4824	0.6035	8.195E-005	612.8
	-30	0.08608	1.565E-003	22.19	0.0006709	0.5767	0.030584198	0.5664	0.6787	7.68E-005	694.5
	-35	7.668	1.572E-003	20.69	0.0006948	0.5771	0.031028472	0.6216	0.6420	7.184E-005	859.1
	-40	1000	1.543E-003	20.63	0.0006994	0.5858	0.034928006	0.6009	0.7206	6.676E-005	835.5
	-45	1	1.399E-003	25.08	0.0007484	0.5588	0.032429991	0.4893	0.8133	8.306E-005	696
	-50	0.1	1.514E-003	23.29	0.0006863	0.5825	0.0354018	0.458	0.8245	8.105E-005	572.9
	-55	1	1.493E-003	23.42	0.0006862	0.5871	0.037564677	0.5387	0.8798	8.01E-005	547.1
	-60	1	1.4E-003	24.65	0.0006614	0.5857	0.035967119	0.547	0.8866	7.964E-005	604.7
	-65	0.01	1.543E-003	21.25	0.000169	0.9321	0.112149022	1.21E004	2.3832	0.0002221	310.7
	-70	0.7308	1.57E-003	21.13	0.0001603	0.9433	0.113882345	1163	2.4063	0.0002256	311.8
	-75	0.1	1.567E-003	21.43	0.0001752	0.9293	0.114553755	124.9	2.4549	0.0002204	304.3
	-80	1	1.53E-003	20.46	0.0004534	0.7764	0.117787008	371.7	2.4099	3.213E018	2.492
	-85	0.01	1.558E-003	20.52	0.0004773	0.7714	0.12117875	5.164E006	2.4866	1.965E017	192.2
	-90	0.8103	1.593E-003	21.72	0.0001589	0.9495	0.117538292	120.1	2.5529	0.0002279	303.6
	-95	0.8345	1.586E-003	21.94	0.0001475	0.9605	0.116518103	110.6	2.5564	0.000225	292
	-100	0.8437	1.58E-003	22.15	0.0001657	0.9449	0.119484761	124.5	2.6466	0.0002299	290.7
	-105	8.533	1.565E-003	22.37	0.0001469	0.9622	0.117345096	111.5	2.6250	0.0002311	278.5

Table S6. The fitted parameters of the EIS data of EG-Pt/pCNTs-60 for HER.

	η (mV)	R_s (Ω)	C_1 (F)	R_1 (Ω)	CPE_2 (mF)	n	C2 (mF)	R_2 (Ω)	$\tau_2/10^{-3}$s	C_2 (F)	R_3 (Ω)
EG-Pt/pCNTs-60	0	7.249	2.331E-007	8.339	0.007469	0.387	0.091955911	16.38	0.7668	0.000703	4.719E009
	-5	7.914	2.16E-007	9.148	0.006941	0.3919	0.096312074	20.29	0.8811	0.0007461	1.625E010
	-10	7.382	2.657E-007	8.136	0.006691	0.4093	0.100265192	22.38	0.8158	0.0007466	9.887E011
	-15	8.397	2.34E-007	8.267	0.007005	0.4229	0.143560147	19.02	1.1868	6.209E-005	4.02E017
	-20	8.461	2.359E-007	9.034	0.007221	0.413	0.149143805	15.97	1.3474	0.0007156	4.814E011
	-25	5.208	2.796E-007	7.555	0.005028	0.5157	0.233081966	14.12	1.7609	0.0007159	7.062E010
	-30	9.421	2.164E-007	9.443	0.007022	0.4338	0.203405895	16.98	1.9208	0.0005882	6.689E018
	-35	9.438	2.463E-007	8.349	0.004658	0.5429	0.302619069	16.76	2.5266	0.0007708	1.374E011
	-40	5.44	3.45E-005	6.985	0.009747	0.4614	0.423307359	0.01	2.9568	7.52E-017	1.093E019
	-45	6.365	4.026E-005	8.368	0.005966	0.5864	0.720395339	0.01002	6.0283	1.38E-012	6.675E010
	-50	5.882	3.238E-007	9.21	0.006514	0.5519	0.663385093	4.742E005	6.1098	2.147E-007	4.765E011
	-55	8.461	3.048E-007	9.743	0.007235	0.5419	0.768592249	2.35E014	7.4884	1.303E-010	4276
	-60	6.025	3.247E-007	9.562	0.005984	0.5897	0.817553309	1.402E013	7.8174	3.78E-010	0.01184
	-65	5.61	3.528E-007	8.35	0.005635	0.6245	0.896895201	0.01331	7.4891	9.802E-019	6.89E017
	-70	7.665	2.81E-007	10.19	0.006933	0.5504	0.795779451	6.078E013	8.1090	7.714E-010	1.233
	-75	9.917	2.466E-007	10.74	0.007217	0.5339	0.77403005	1.582E018	8.3131	3.197E-011	6.356
	-80	8.833	2.269E-007	10.89	0.007763	0.5251	0.831115262	3.574E006	9.0508	2.233E-009	7.03E012
	-85	8.233	2.515E-007	11.2	0.007321	0.5368	0.845839561	4.641	9.4734	1.127E-020	8.064E012
	-90	7.961	2.694E-007	10.74	0.006991	0.5549	0.876159152	1.098E013	9.4099	3.127E-009	4.056
	-95	8.663	2.825E-007	10.28	0.006724	0.5783	0.95823472	4.094E011	9.8507	46.39	3.182E005
	-100	7.996	2.347E-007	10.72	0.006686	0.5809	0.998498866	1.874E017	10.7039	3.388E-011	5.273E019
	-105	8.574	2.327E-007	10.82	0.006828	0.5697	0.954280721	1.385E005	10.3253	1.326E-020	2.307E012

Table S7. The fitted parameters of the EIS data of EG-Pt/pCNTs-100 for HER.

	η (mV)	R_s (Ω)	C_1 (F)	R_1 (Ω)	CPE_2 (mF)	n	C_2 (mF)	R_2 (Ω)	$\tau_2/10^{-3}$s	C_φ (F)	R_3 (Ω)
EG-Pt/pCNTs-100	0	1	1.341E-006	18.46	0.0001582	1	0.1582	96.86	2.9204	0.0001991	195.3
	-5	1000	1.343E-006	18.4	0.00016	0.9997	0.159720417	93.3	2.9389	0.0002066	179.2
	-10	0.01	1.152E-006	20.02	0.0001474	1	0.1474	91.04	2.9509	0.01503	514.5
	-15	0.01	1.34E-006	18.66	0.0001583	1	0.1583	967.9	2.9539	0.0001925	204
	-20	10	1.164E-006	20.62	0.0001442	1	0.1442	84.52	2.9734	0.0001282	442.9
	-25	0.01	1.347E-006	18.28	0.0001633	1	0.1633	89.29	2.9851	2.212E-005	154
	-30	0.01	1.186E-006	20.04	0.0001706	0.9792	0.151214715	111.1	3.0303	0.0001361	46.56
	-35	0.01	1.172E-006	20.67	0.0001556	0.9926	0.149082432	122	3.0815	1.331	6.485E008
	-40	0.01	1.323E-006	18.56	0.0001654	1	0.1654	108.7	3.0698	0.0002017	1.98
	-45	0.01	1.342E-006	18.85	0.0001598	1	0.1598	981.1	3.0122	0.0001885	209.8
	-50	10	1.339E-006	18.72	0.0001664	1	0.1664	82.97	3.1150	0.0002564	109.4
	-55	100	1.322E-006	19.01	0.0001668	1	0.1668	92.15	3.1709	0.0002525	121.3
	-60	0.01	1.303E-006	19.44	0.0001627	1	0.1627	83.96	3.1629	2.13E-006	140.8
	-65	0.01	1.34E-006	18.79	0.0001685	1	0.1685	91.25	3.1661	0.0002435	1.329
	-70	0.01	1.192E-006	20.63	0.0001527	1	0.1527	95.62	3.1502	0.01296	373.6
	-75	100	1.336E-006	19.25	0.0001669	1	0.1669	95.16	3.2128	0.0002196	150
	-80	100	1.235E-006	20.84	0.0001599	0.9938	0.154309858	80.85	3.2158	0.0002035	155.4
	-85	0.01	1.315E-006	19.67	0.0001643	1	0.1643	90.15	3.2318	2.14E-005	153.4
	-90	1	1.343E-006	19.23	0.0001699	1	0.1699	92.47	3.2672	0.0002548	125.7
	-95	0.01	1.318E-006	19.78	0.0001672	1	0.1672	84.67	3.3072	0.002366	128
	-100	0.01	1.18E-006	20.08	0.0003869	0.8551	0.169868359	8085	3.4110	1E-020	0.01
	-105	0.01	1.197E-006	20.06	0.0003488	0.8774	0.174358523	5.976E005	3.4976	1.684E011	253.1

Table S8. The fitted parameters of the EIS data of EG-Pt/pCNTs-200 for HER.

	η (mV)	R_s (Ω)	C_1 (F)	R_1 (Ω)	CPE_2	n	C2 (mF)	R_2 (Ω)	$\tau_2/10^{-3}$s	C_φ (F)	R_3 (Ω)
EG-Pt/pCNTs-200	0	0.1	2.509E-007	77.53	0.000186	0.8995	0.1158	314.5	8.9802	7.875E-005	645.5
	-5	1	2.311E-007	79.5	0.0001845	0.8974	0.1139	216.4	9.0516	8.811E-005	508.2
	-10	1	2.651E-007	74.8	0.0002756	0.8365	0.12905	1288	9.6533	7.571E017	5.808E005
	-15	0.01	2.399E-007	78.65	0.0002919	0.8287	0.1338	0.1089	10.5226	1E-020	4.524
	-20	1000	2.854E-007	78.4	0.0001413	1	0.1413	676	11.0779	0.0002488	1E016
	-25	0.01	2.544E-007	81.38	0.0001397	1	0.1397	7.413E004	11.3688	0.0002043	3E004
	-30	1	2.6E-007	81.06	0.0001405	1	0.1405	738.7	11.3889	0.000214	2.398E012
	-35	1000	2.734E-007	80.14	0.0001431	1	0.1431	686.7	11.4680	0.0002578	3.194E009
	-40	0.01	2.558E-007	81.07	0.0001409	1	0.1409	626.9	11.4228	0.0002088	773.9
	-45	0.01	2.535E-007	81.49	0.00014	1	0.14	615.3	11.4086	0.0001972	850.9
	-50	1	2.445E-007	83.12	0.000139	1	0.139	697.7	11.5537	0.0001968	2946
	-55	0.01	2.501E-007	82.2	0.0001412	1	0.1412	585.7	11.6066	0.00021	653.6
	-60	0.01	2.388E-007	82.28	0.0001397	1	0.1397	545.7	11.4945	0.0001986	636.5
	-65	101.5	2.319E-007	82.85	0.0001412	1	0.1412	526.3	11.6984	0.0002069	577
	-70	0.01	2.354E-007	83.03	0.0001399	1	0.1399	533.6	11.6159	0.0002031	59.74
	-75	0.01	2.433E-007	83.31	0.0001426	0.9981	0.1414	601.9	11.7802	0.0002261	760.5
	-80	0.01	2.646E-007	80.99	0.0001451	1	0.1451	693	11.7516	0.003388	1434
	-85	10	2.696E-007	84.4	0.0001437	1	0.1437	676.8	12.1283	0.000269	3.976E005
	-90	0.01	2.612E-007	83.81	0.0001456	1	0.1456	560.8	12.2027	0.0002636	486.1
	-95	0.01	2.658E-007	80.43	0.0001767	0.9663	0.1523	9.57E004	12.2526	1.991E-016	0.2032
	-100	0.01	2.417E-007	82.18	0.0001892	0.9478	0.1504	1057	12.3622	4.535E-014	100
	-105	100	2.444E-007	82.22	0.0001881	0.9493	0.1505	1081	12.3784	7.996E006	0.02252

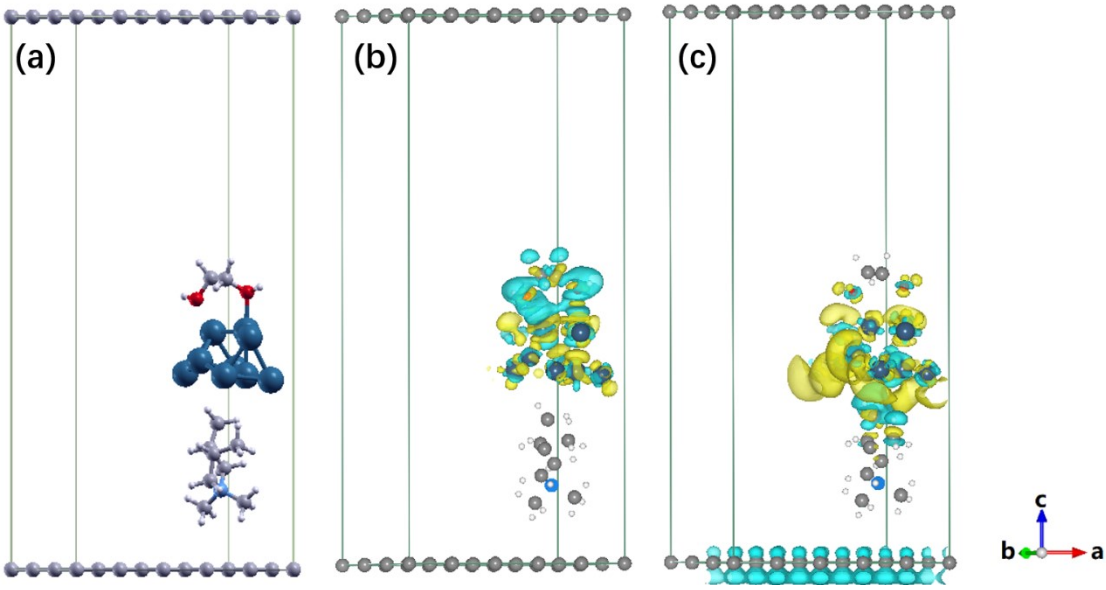

Fig.S18 Optimized structure (a) and difference charge density of (b) $\Delta\rho_1 = \rho_{\text{EG-Pt(111)-substrate}} - \rho_{\text{EG}} - \rho_{\text{Pt(111)-substrate}}$) and (c) $\Delta\rho_2 = \rho_{\text{EG-Pt(111)-substratre}} - \rho_{\text{EG-Pt(111)}} - \rho_{\text{substratre}}$ for the constructed model system containing one EG molecule, Pt(111) with 9 metal atoms, one unit of PDDA polymer electrolyte and periodically repeating monolayer graphene with 5 3 supercell, and the yellow and light blue regions represent positive charge accumulation and depletion, respectively. The C, N, O, H and Pt atoms are shown in grey, blue, red, white and grey-blue colors, respectively.

Table S9 Comparison of HER performance in alkaline media for EG-Pt/pCNTs-100 with the state-of-the-art HER catalysts.

Catalyst	η_{10} mV	Tafel slope mV/dec	Catalyst loading mg/cm^2	Nobel metal loading mg/cm^2	Ref
CoP/CoMoP	34	33		0	13
PtNi-O/C	39.8	38.8		0.0051	14
IrP_2@NC	28	50	0.7	0.077	15
Pt / NiO @ Ni / NF	34	39	2.0	0.092	16
20 wt% Pt/$Ni(HCO_3)_2$	44	40		0.04	17
g-MoC_{1-x}/Pt nanoparticles	67	55	2	0.054~0.06	18
Pt on edgerich WS_2	45	65	0.64		19
Pt–$Co(OH)_2$ / CC	32	70	6.9 (Pt-$Co(OH)_2$)	0.39(Pt-$Co(OH)_2$) without CC	20
W_2C@CNT-S	148	56	0.28		21
Ni−Mo_xC/NC	161	168.7	0.86		22
EG-Pt/pCNTs-100	175	137	0.278	0.006	This work

Table S10 Comparison of HER performance in alkaline media for EG-Pt/pCNTs-100 with the state-of-the-art HER catalysts.

Catalyst	η_{10} mA	Tafel slope mV/dec	Catalyst loading mg/cm^2	Nobel metal loading mg/cm^2	Ref
CoP/CoMoP	72	50		0	13
hcp-Ru@ NC-700	27.5	37	0.28	0.0476	23
$Pt_{1.8}MoS_2$	80	48			24
IrP_2@NC	8	28	0.7	0.077	15
CPt @ ZIF-6	50	27.1	0.26	0.013	25
Pt/MoS_2 -80	31	52	3	0.066	26
Pt@CoS	28	31			27
g-MoC_{1-x}/Pt nanoparticles	30	31	2	0.054~0.06	18
10Pt@HN-BC	-47	-35		0.012	28
$PtNi_5$-0.3	28	19.2			29
Pt-Ag/SiNW-3	135	70	0.170	0.007	30
Pt/MoS_2	67,4	76.2		3.0 wt%	31
PtRu@RFCS	19.7	27.2	0.354	0.00071Pt 0.0177Ru	32
EG-Pt/pCNTs-100	29	35	0.278	0.006	This work

References

1 J. Y. Li, H. X. Liu, W. Y. Gou, M. K. Zhang, Z. M. Xia, S. Zhang, C. R. Chang, Y. Y. Ma, Y. Q. Qu, *Energ. Environ. Sci.* 2019, **12**, 2298-2304.

2 P. Giannozzi, S. Baroni, N. Bonini, M. Calandra, R. Car, C. Cavazzoni, D. Ceresoli, G. L. Chiarotti, M. Cococcioni, I. Dabo, A. Dal Corso, S. de Gironcoli, S. Fabris, G. Fratesi, R. Gebauer, U. Gerstmann, C. Gougoussis, A. Kokalj, M. Lazzeri, L. Martin-Samos, N. Marzari, F. Mauri, R. Mazzarello, S. Paolini, A. Pasquarello, L. Paulatto, C. Sbraccia, S. Scandolo, G. Sclauzero, A. P. Seitsonen, A. Smogunov, P. Umari, R. M. Wentzcovitch, *J. Phys. Condens. Matter.* 2009, **21**, 395502.

3 P. Giannozzi, O. Andreussi, T. Brumme, O. Bunau, M. B. Nardelli, M. Calandra, R. Car, C. Cavazzoni, D. Ceresoli, M. Cococcioni, N. Colonna, I. Carnimeo, A. Dal Corso, S. de Gironcoli, P. Delugas, R. A. DiStasio, A. Ferretti, A. Floris, G. Fratesi, G. Fugallo, R. Gebauer, U. Gerstmann, F. Giustino, T. Gorni, J. Jia, M. Kawamura, H. Y. Ko, A. Kokalj, E. Kucukbenli, M. Lazzeri, M. Marsili, N. Marzari, F. Mauri, N. L. Nguyen, H. V. Nguyen, A. Otero-de-la-Roza, L. Paulatto, S. Ponce, D. Rocca, R. Sabatini, B. Santra, M. Schlipf, A. P. Seitsonen, A. Smogunov, I. Timrov, T. Thonhauser, P. Umari, N. Vast, X. Wu, S. Baroni, *J. Phys-Condens. Mat.* 2017, **29**, 465901.

4 A. Dal Corso, *Phys. Rev. B* 2012, **86**, 085135.

5 K. B. J. P. Perdew, M. Ernzerhof, *Phys. Rev. Lett.* 1996, **77**, 3865-3868.

6 J. D. P. H. J. Monkhorst, *Phys. Rev. B* 1976, **13**, 5188-5192.

7 S. Grimme, *J. Comput. Chem.* 2006, **27**, 1787-1799.

8 V. Barone, M. Casarin, D. Forrer, M. Pavone, M. Sambi, A. Vittadini, *J. Comput. Chem.* 2009, **30**, 934-939.

9 O. Andreussi, I. Dabo, N. Marzari, *J. Chem. Phys.* 2012, **136**, 064102.

10 A. Kokalj, *J. Mol. Graph. Model.* 1999, **17**, 176-179, 215-216.

11 A. Kokalj, *Comput. Mater. Sci.* 2003, **28**, 155-168.

12 K. Momma, F. Izumi, *J. Appl. Crystallogr.* 2011, **44**, 1272-1276.

13 X. K. Huang, X. P. Xu, X. X. Luan, D. J. Cheng, *Nano Energy* 2020, **68**, 104332.

14 Z. P. Zhao, H. T. Liu, W. P. Gao, W. Xue, Z. Y. Liu, J. Huang, X. Q. Pan, Y. Huang, *J. Am. Chem. Soc.* 2018, **140**, 9046-9050.

15 Z. H. Pu, J. H. Zhao, I. S. Amiinu, W. Q. Li, M. Wang, D. P. He, S. C. Mu, *Energ. Environ. Sci.* 2019, **12**, 952-957.

16 Z. J. Chen, G. X. Cao, L. Y. Gan, H. Dai, N. Xu, M. J. Zang, H. B. Dai, H. Wu, P. Wang, *Acs Catal.* 2018, **8**, 8866-8872.

17 M. M. Lao, K. Rui, G. Q. Zhao, P. X. Cui, X. S. Zheng, S. X. Dou, W. P. Sun, *Angew. Chem. Int. Edit.* 2019, **58**, 5432-5437.

18 H. J. Song, M. C. Sung, H. Yoon, B. Ju, D. W. Kim, *Adv. Sci.* 2019, **6**, 1802135.

19 K. Tang, X. F. Wang, Q. Li, C. L. Yan, *Adv. Mater.* 2018, **30**, 1870047.

20 Z. C. Xing, C. Han, D. W. Wang, Q. Li, X. R. Yang, *Acs Catal.* 2017, 7, 7131-7135.

21 Y. Hu, B. Yu, W. X. Li, M. Ramadoss, Y. F. Chen, *Nanoscale* 2019, **11**, 4876-4884.

22 D. Das, S. Santra, K. K. Nanda, *Acs Appl. Mater. Inter.* 2018, **10**, 35025-35038.

23 Y. T. Li, L. A. Zhang, Y. Qin, F. Q. Chu, Y. Kong, Y. X. Tao, Y. X. Li, Y. F. Bu, D. Ding, M. L. Liu, *Acs Catal.* 2018, **8**, 5714-5720.

24 X. Y. Chia, N. A. A. Sutrisnoh, M. Pumera, *Acs Appl. Mater. Inter.* 2018, **10**, 8702-8711.

25 Y. D. Qin, X. Y. Han, S. Gadipelli, J. Guo, S. J. Wu, L. Q. Kang, J. Callison, Z.

X. Guo, *J. Mater. Chem. A* 2019, **7**, 6543-6551.

26 W. N. Ren, H. F. Zhang, C. W. Cheng, *Electrochim. Acta* 2017, **241**, 316-322.

27 A. Mosallanezhad, C. Wei, P. A. Koudakan, Y. Fang, S. Niu, Z. Bian, B. Liu, T. Huang, H. Pan, G. Wang, *Applied Catalysis B: Environmental* 2022, **315**, 121534.

28 Y. Zhang, J. Tan, F. F. Wen, Z. F. Zhou, M. Zhu, S. X. Yin, H. G. Wang, *Int. J. Hydrogen Energ.* 2018, **43**, 6167-6176.

29 C. Zhang, X. Liang, R. Xu, C. Dai, B. Wu, G. Yu, B. Chen, X. Wang, N. Liu, *Adv. Fun. Mater.* 2021, **31**, 2008298.

30 W. Shen, B. Wu, F. Liao, B. B. Jiang, M. W. Shao, *Int. J. Hydrogen. Energ.* 2017, **42**, 15024-15030.

31 A. Shan, X. Teng, Y. Zhang, P. Zhang, Y. Xu, C. Liu, H. Li, H. Ye, R. Wang, *Nano Energy* 2022, **94**, 106913.

32 K. Li, Y. Li, Y. M. Wang, J. J. Ge, C. P. Liu, W. Xing, *Energ. Environ. Sci.* 2018, **11**, 1232-1239.